ORIGINAL ARTICLE　　　　　　　　　　　　　　　　　　　**Open Access**

The BRD4 inhibitor JQ1 protects against chronic obstructive pulmonary disease in mice by suppressing NF-κB activation

Yan Liu[1], Zhi-Zhen Huang[2], Li Min[3], Zhi-Feng Li[4] and Kui Chen[5]

[1]Department of Respiratory and Critical Care Medicine, [2]Department of Stomatology, [3]Department of Critical Care Medicine, [4]Department of Orthopedics, Taihe Hospital, Hubei University of Medicine and [5]Department of Emergency Medicine, Affiliated Dongfeng Hospital, Hubei University of Medicine, Shiyan, Hubei, China

Summary. Objective. To examine the effect of the BRD4 inhibitor JQ1 on mice with chronic obstructive pulmonary disease (COPD) via NF-κB.

Methods. COPD models constructed by exposure to cigarette smoke and intratracheal instillation of lipopolysaccharides (LPS) in mice were treated with JQ1 (15, 25 or 50 mg/kg). HE staining was performed to observe histopathological changes in the lung tissues. Enzyme-linked immunosorbent assays (ELISAs) were used to measure the levels of IL-10, IFN-γ, IL-17, IL-1β, IL-6, TNF-α, MMP-2, MMP-9, MDA, SOD, T-AOC and HO-1, and gelatin zymography assays were used to examine MMP-2 and MMP-9 activity. A TransAM™ NF-κB p65 detection kit was used to test NF-κB p65/DNA binding activity. Western blotting was conducted to analyze NF-κB p65 in the nucleus and its acetylation.

Results. JQ1 dose-dependently improved the histopathological changes in the lung tissues and decreased the mean linear intercept (MLI), destructive index and inflammatory score of the mice with COPD. The mice with COPD showed increased levels of MMP-2, MMP-9, IFN-γ, IL-17, IL-1β, IL-6 and TNF-α with decreased IL-10 level; these changes were reversed by JQ1 in a dose-dependent manner. In addition, JQ1 reduced the MDA level and increased the SOD, HO-1 and T-AOC levels in mice with COPD, with suppression of NF-κB p65 expression in the nucleus, NF-κB/p65 (Lys310) acetylation and NF-κB p65/DNA binding activity in the lung tissues.

Conclusion. The BRD4 inhibitor JQ1 can downregulate MMP-2 and MMP-9 expression, reduce inflammatory responses, and alleviate oxidative stress in mice with COPD, and this mechanism might be related to the inhibition of NF-κB.

Key words: Chronic obstructive pulmonary disease, BRD4, JQ1, NF-κB

Introduction

Chronic obstructive pulmonary disease (COPD) is a complicated long-term inflammatory lung disease characterized by irreversible and progressive airflow obstruction and alveolar destruction, and the abnormal inflammatory response of the lungs to noxious gases and particles has been regarded as a crucial cause of COPD (Ge et al., 2019). The main pathological features of lung tissues in patients with COPD include chronic airway inflammation, accompanied by infiltration of various inflammatory cells and airway remodeling, severely affecting human health, and this disease will become the third leading cause of death worldwide by 2030 (Ding et al., 2018; Tang and Ling, 2019). With the increase in the aging population, the morbidity and mortality of COPD continue to increase year by year (Fang et al., 2018). Currently, long-acting muscarinic antagonists, inhaled corticosteroids, or long-acting β2-agonists have been recommended as first-line drugs for symptomatic therapy of COPD (Rodrigo and Neffen, 2017). However, only 40% of COPD patients were relatively satisfied with these drugs (Sakai et al., 2017), indicating the urgent need for alternative treatments for COPD.

Bromodomain-containing protein 4 (BRD4) belongs to the bromodomain and extraterminal (BET) family of proteins, which contains two bromodomains and one extraterminal domain (Sakaguchi et al., 2018). As a transcription coactivator and epigenetic regulator, BRD4

plays a critical role in inflammation-related diseases (Park et al., 2018). Notably, the level of BRD4 was significantly upregulated in patients with COPD or cigarette smoke extract (CSE)-treated human bronchial epithelial (Beas-2B) cells *in vitro*, as reported by previous studies (Tang et al., 2019). JQ1 was shown to act specifically against the BET protein, particularly BRD4, which is an active isomer that selectively interacts with the BD1 and BD2 domains of BRD4 and disrupts the binding of BRD4 to acetylated lysines (Lv et al., 2018; Qu et al., 2018; Sakaguchi et al., 2018). Evidence has also demonstrated the therapeutic role of Brd4 inhibition with JQ1 in several disorders, including cancers (da Motta et al., 2017; Leal et al., 2017), Huntington's disease (HD) (Kedaigle et al., 2020), liver fibrosis (Hassan et al., 2019), cisplatin-induced nephrotoxicity (Sun et al., 2018), and mechanical injury-induced corneal scarring (Qu et al., 2018), as well as its potential in inhibiting the development and progression of inflammation-related diseases, such as inflammation and cardiovascular diseases, in animal models. For example, Wang et al. revealed that JQ1 could significantly downregulate lipopolysaccharides (LPS)-induced transcription of inflammatory cytokines both *in vitro* and *in vivo* (Wang et al., 2018). Leal AS et al. demonstrated that JQ1 suppressed the production of various inflammatory cytokines, including IL-6, CcL2, and GM-CSF, in both immune and pancreatic cancer cells (Leal et al., 2017). In addition, JQ1 inhibited the profibrotic transcriptional networks in heart failure (HF) and constitutes a potential option for clinical HF treatment (Duan et al., 2017). Since COPD and HF share similar pathological gene regulatory programs, such as innate inflammatory and profibrotic transcriptional networks (Xiao et al., 2018), we naturally hypothesized that JQ1 might be a promising drug for COPD treatment. Furthermore, BRD4 dysfunction can result in an interaction with nuclear factor kappa-B (NF-κB), thereby mediating the development of autoimmune diseases and inflammation (Mumby et al., 2017). NF-κB, as a powerful protein complex controlling the transcription of DNA, plays an important role in early inflammation, and its activation can lead to the release of inflammatory mediators, as well as the proliferation and activation of airway smooth muscle cells and fibroblasts; these changes can cause the hypertrophy and hyperplasia of airway smooth muscles and the accumulation of fibroblasts, eventually promoting the development and progression of COPD (Mercken et al., 2011; Yuan et al., 2018). To determine whether JQ1 plays a role in COPD by regulating NF-κB, the present study established COPD models in mice by using cigarette smoke exposure and intratracheal instillation of LPS. Then, different dosages of the BRD4 inhibitor JQ1 (including 15 mg/kg, 25 mg/kg and 50 mg/kg) were used for COPD treatment, and mice were observed for histopathological conditions, oxidative stress and inflammation, as well as the expression level of NF-κB in lung tissues.

Materials and methods

Ethical statement

All animal experiments in this study were performed in accordance with local regulations on the management and use of experimental animals, complying with the requirements of animal ethics, and abiding by the Guide for the Care and Use of Laboratory Animals issued by the US National Institutes of Health (NIH) (Mason and Matthews, 2012).

Animal grouping

The experimental animals used in this study were 60 SPF-grade male BALB/c mice (aged 6-7 weeks old and weighing 20.0±2.0 g), which were purchased from the Institute of Laboratory Animal Science, Chinese Academy of Medical Sciences (CAMS) & Peking Union Medical College (PUMC). The mice were randomized to six groups: the normal group, 50 mg/kg JQ1 group, COPD group, 15 mg/kg JQ1+COPD group, 25 mg/kg JQ1+COPD group, and 50 mg/kg JQ1+COPD group, with 10 mice in each group.

Establishment of COPD models

All mice except for those in the normal group were passively exposed to cigarette smoke and treated intratracheally with LPS to establish COPD models according to previous studies (Zhang et al., 2012a; Wang et al., 2014, 2017). In brief, mice were intraperitoneally injected with 10% chloral hydrate (300 mg/kg) for anesthesia, fixed on the anatomical plate, and instilled intratracheally with LPS (200 μg/200 μL) on day 1 and day 14. After LPS instillation, the mice were spanned for 10-20 s in an upright position to evenly distribute LPS in the lung. On days 2~13 and 15~28, the mice were exposed to cigarette smoke (30 min/time, 10 cigarettes/day, Hongjinlong, Hubei China Tobacco Industry Co., Ltd., Wuhan, China) in a closed organic glass box (80×60×50 cm). Each cigarette contains 9 mg tar, 0.7 mg nicotine and 12 mg carbon monoxide. From day 29 on, mice in the JQ1 treatment groups were intraperitoneally injected with JQ1 (15 mg/kg, 25 mg/kg, 50 mg/kg) for 20 consecutive days. Mice in the normal group and COPD group were injected with an equal volume of normal saline. A flow chart of the animal experiments is shown in Fig. 1.

Lung function test

The lung function of the mice (n=10 in each group) was assessed using a small animal spirometer (Buxco Electronics, Inc., Wilmington, NC, USA) according to the manufacturer's protocol. The efficacy of JQ1 in mice with COPD was determined via airway resistance (Raw), lung dynamic compliance (Cdyn), peak expiratory flow

(PEF) and inspiratory time/expiratory time (Ti/Te).

Sample collection

Mice were intraperitoneally injected with 1% pentobarbital sodium (40 mg/kg) for anesthesia, and abdominal aortic blood (8-10 ml) was collected after execution. The trachea and lung were exposed by a mid-neck incision, a transverse incision was made in the lower trachea, and a 12-gauge needle (with polished tip) was inserted from the trachea incision to ligate the right main bronchus. Sterile normal saline precooled to 4°C was taken and slowly instilled into the left lung for lavage. After each instillation, the lavage was collected with a recovery rate of approximately 80~90%. The recovered BALF was centrifuged, and the supernatant fraction was stored at -80°C for further cytokine analysis. A hematocytometer (Neubauer chamber) was used for counting total cells. The differential cell analyses were performed using a cytocentrifuge (Cytospin) preparation and stained with the May-Grünwald-Giemsa method. Right lung tissues were taken for fixation in formaldehyde, routine embedding with paraffin, slicing of 4 μm serial sections, baking and HE staining, and finally observation of histopathology under a light microscope. The remaining lung tissues, BALF, and serum were preserved at -80°C for subsequent quantification of inflammatory cytokines (IL-10, IFN-γ, IL-17, IL-1β, IL-6, TNF-α), the measurement of serum levels of MMP-2 and MMP-9, and the determination of activities of MDA, SOD, T-AOC, and HO-1, following the manufacturer's protocol (R&D Systems, Minneapolis, MN, USA). Nuclear proteins were extracted prior to testing NF-κB binding activity using a TransAM NF-κB p65 activity assay kit (Active motif, Belgium).

Hematoxylin and eosin (H&E) staining

Paraffin-embedded sections (n=10 in each group) were routinely deparaffinized in water, stained with hematoxylin for 10 min at room temperature, and rapidly rinsed with tap water for 30-60 s. After differentiation with 1% hydrochloric ethanol for 1 min and rinsing with tap water again for 1 min, the tissues were stained with eosin for 5-10 min at room temperature, dehydrated with gradient ethanol (1 min/time), hyalinized with xylene twice (1 min/time) and mounted with neutral gum prior to observation and photographing under a light microscope. The mean linear intercept (MLI) refers to the value of the total length of lines drawn across lung sections divided by the number of alveoli intercepts at the intersection point of two horizontal and vertical lines. The destructive index (DI) was defined as the percentage of destroyed alveoli in all the alveoli counted per section. Inflammatory infiltration was graded as follows: score 0 (absent); score 1 (minimal), with a single layer clustering of inflammatory cells; score 2 (moderate), with localized clustering of inflammatory cells; and score 3 (abundant), with large clusters of inflammatory cells.

Gelatin zymography assay

Proteins were loaded for electrophoresis (20 mA/gel), and electrophoresis ended when bromophenol

Fig. 1. Flow chart of animal experiments.

blue ran out of the gel front. The gel was washed with buffer and soaked in 10 ml of incubation buffer for 1-5 h of incubation at room temperature or at 37°C. Then, incubation buffer was removed from the gel, and the gel was stained in Coomassie Brilliant Blue solution. The location and scope of transparent areas indicate the location and activity of MMP-2 and MMP-9 (n=10 in each group).

Western blotting

Total nuclear proteins were extracted with extraction reagent, quantified for total protein concentration by using the BCA method, and separated by electrophoresis with 10% polyacrylamide gel. Protein extracts were transferred onto polyvinylidene difluoride membranes (PVDF) through a semidry transfer system (Bio-Rad, USA). Membranes were blocked with skim milk at room temperature, rinsed with PBST buffer, and incubated with NF-$\varkappa$B p65 antibody (ab207297, 1:30, Abcam, USA), acetyl-NF-$\varkappa$B p65 antibody (ab19870, 1/500, Abcam, USA) and TATA binding protein TBP antibody-nuclear loading control (ab63766, 1 μg/ml, Abcam, USA) for 1 h at room temperature. After washing with PBST (5 min×3 times), the membranes were incubated with secondary antibodies for 1 h at room temperature. After necessary washes with PBST buffer (5 min×3 times), horseradish peroxidase (HRP) substrate (Bio-Rad) was used for reactive band visualization of target proteins. The relative target protein content of samples is shown as the gray value ratio of target protein to TATA-binding protein (TBP) (n=10 in each group).
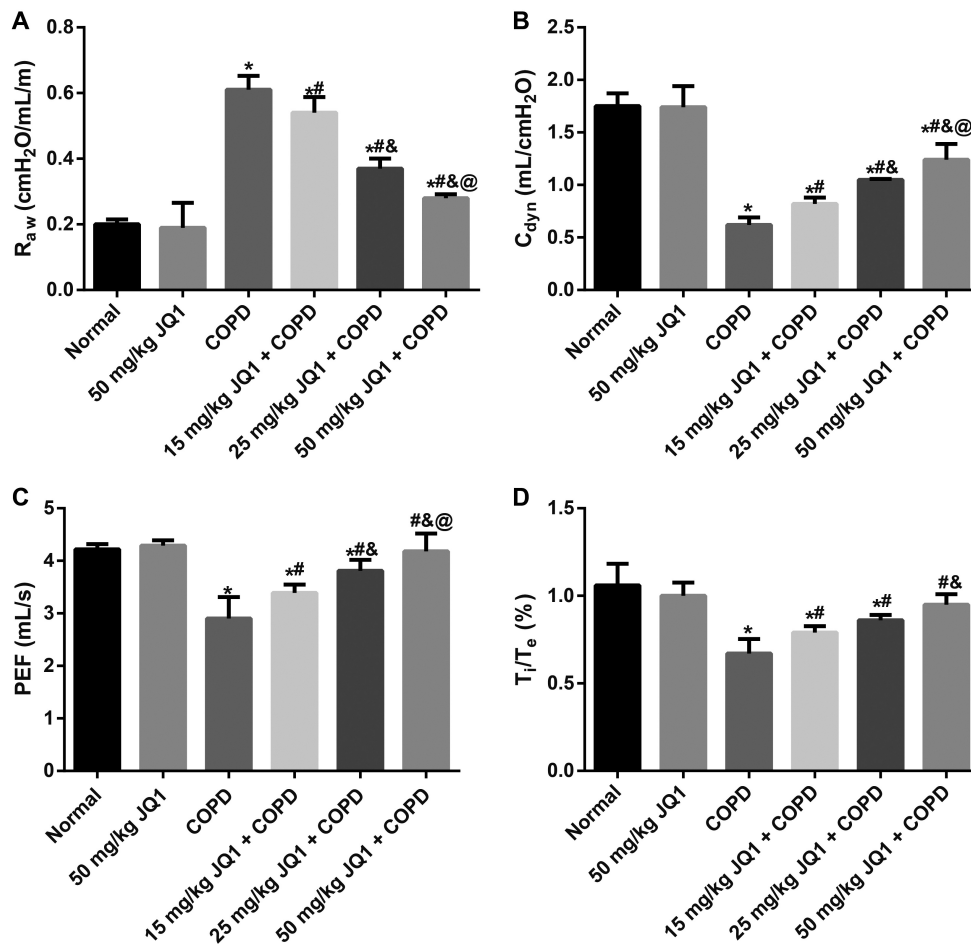
Statistical analysis

All data were analyzed by using the statistical software SPSS 21.0 (SPSS, Inc., Chicago, IL, USA). Multiple-group comparisons of measurement data were performed by using one-way ANOVA followed by post hoc Tukey's test. Statistical significance was indicated by $P<0.05$.

Results

JQ1 improves the lung function of mice with COPD

No mice died during the course of this experiment.

Fig. 2. JQ1 improves the lung function of COPD mice. **A.** Raw (airway resistance). **B.** Cdyn (lung dynamic compliance). **C.** PEF (peak expiratory flow). **D.** Ti/Te (inspiratory time/expiratory time). *: $P<0.05$ compared with the normal group and the 50 mg/kg JQ1 group; #: $P<0.05$ compared with the COPD group; &: $P<0.05$ compared with the 15 mg/kg JQ1 + COPD group; @: $P<0.05$ compared with the 25 mg/kg JQ1 + COPD group.
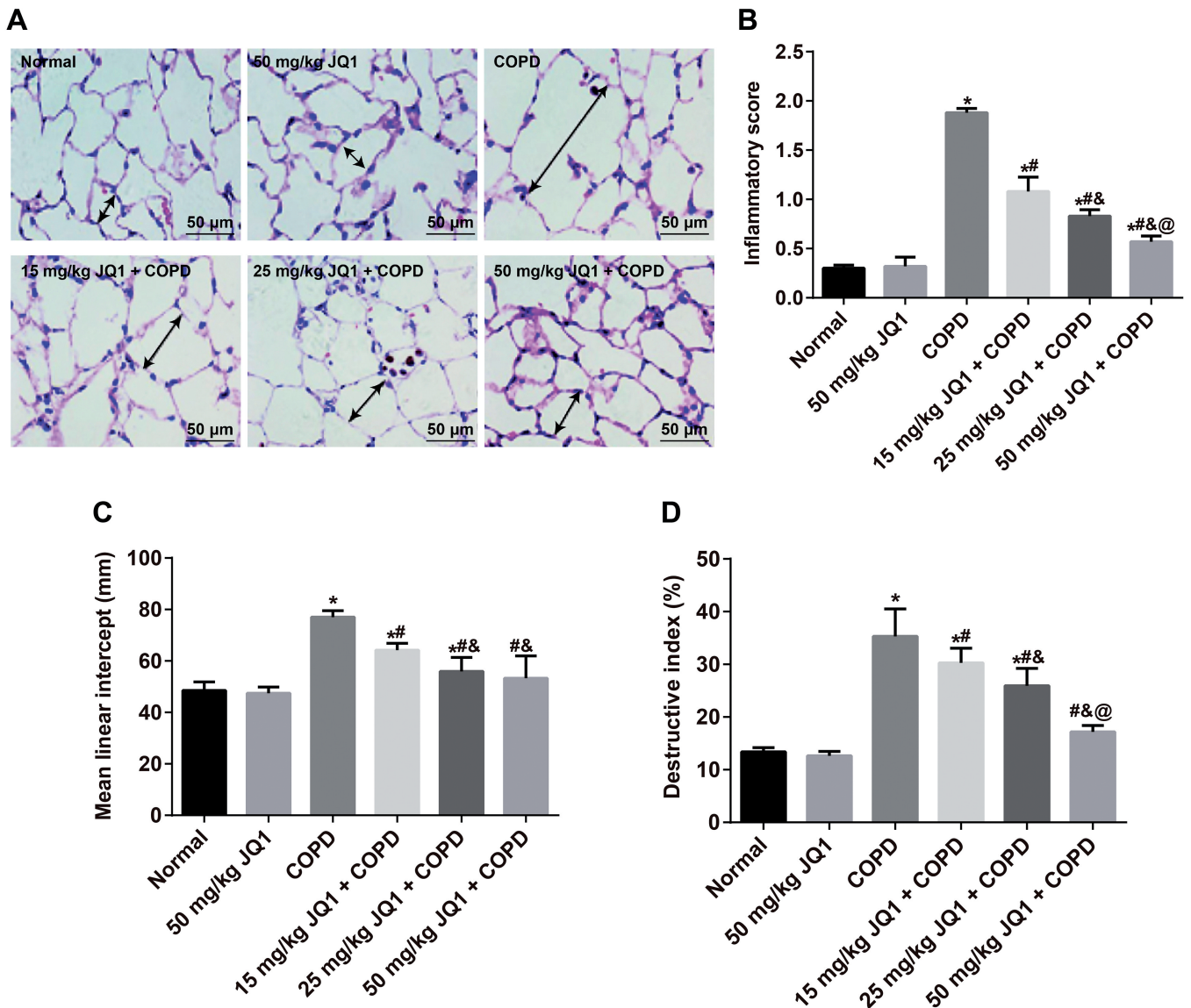
In addition, JQ1 dose-dependently increased the C_{dyn}, PEF and T_i/T_e of the mice with COPD with increased R_{aw} (all $P<0.05$). However, no significant difference was found in R_{aw}, C_{dyn}, PEF and T_i/T_e between the normal group and the JQ1 group (all $P>0.05$, Fig. 2).

JQ1 improves histopathological changes in the lung tissues of the mice with COPD

As shown by the results of HE staining (Fig. 3A), the mice in the normal group had no obvious degenerative necrosis of bronchial epithelial cells and no inflammatory cells, while the mice in the COPD group had emphysema and enlarged alveoli. In contrast, the COPD-related emphysema and alveolar enlargement of the mice in the JQ treatment groups were alleviated. According to the results of the quantification test (Fig. 3B-D), compared with the normal group, the COPD group had an increased mean linear intercept (MLI), destructive index and inflammatory score; however, decreases in the above three indexes were found in the mice from the JQ1 groups with different treatment concentrations compared with the mice in the COPD group, and these parameters decreased more

Fig. 3. JQ1 improves histopathological changes in lung tissues in COPD mice. **A.** Data are representative images of histological changes in lung tissues using HE staining; arrow indicates alveolar enlargement. **B-D.** Comparison of inflammatory score **(B)**, destructive index **(C)** and mean linear intercept (MLI, **D**) among the groups; *: $P<0.05$ compared with the normal group and 50 mg/kg JQ1 group; #: $P<0.05$ compared with the COPD group; &: $P<0.05$ compared with the 15 mg/kg JQ1 + COPD group; @: $P<0.05$ compared with the 25 mg/kg JQ1 + COPD group.

significantly with the increase in JQ1 (all P<0.05).

Effects of JQ1 on MMP-2 and MMP-9 activities in the mice with COPD

A gelatin zymography assay was used to quantify the activities of MMP-2 and MMP-9 (Fig. 4A-B). Compared with the mice in the normal group, those in the COPD group had significantly increased MMP-2 and MMP-9 activities in lung tissues (all P<0.05). Compared with the COPD group, the JQ1 treatment groups showed apparent reductions in the MMP-2 and MMP-9 activities in lung tissues (all P<0.05). No obvious difference was observed between the 50 mg/kg JQ1 + COPD group and the normal group in MMP-2 and MMP-9 activities (all P>0.05). Moreover, we found significant upregulation of

the MMP-2 and MMP-9 levels in the serum of the mice with COPD, which can be inhibited by JQ1 treatment in a dose-dependent manner (all P<0.05, Fig. 4C).

JQ1 reduces leukocytes and inflammatory cytokines in the BALF of the mice with COPD

The data obtained showed that the mice in the COPD group presented a significant increase in total leukocyte influx in BALF with an enhanced number of macrophages, neutrophils, and lymphocytes compared with the mice in the normal group, and these parameters were reduced dose-dependently after treatment with JQ1 (Fig. 5A-D). As illustrated by ELISAs (Fig. 5E-J), the inflammatory cytokines IFN-γ, IL-17, IL-1β, IL-6 and TNF-α were upregulated in the BALF of the mice with
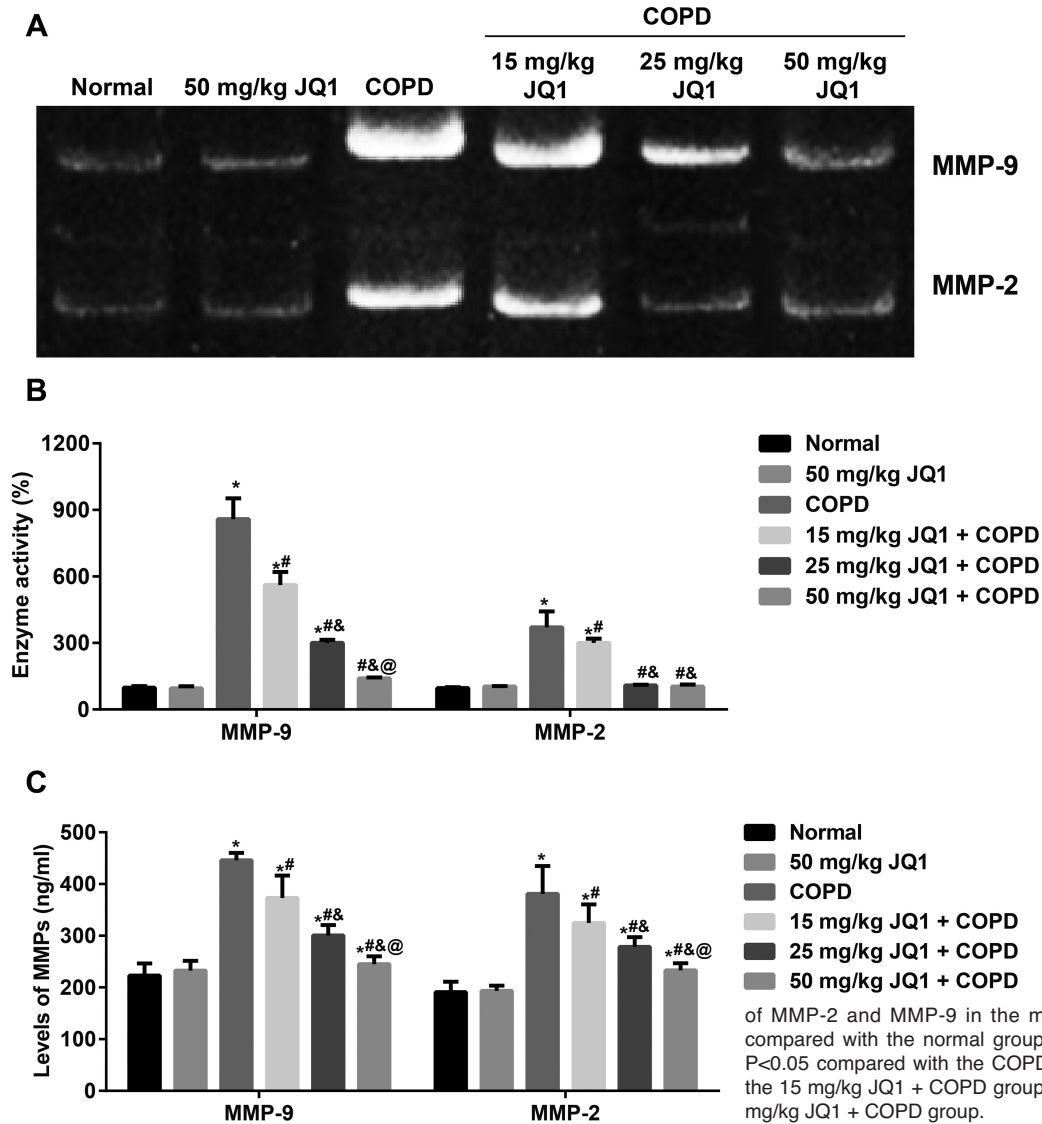

Fig. 4. Effects of JQ1 on MMP-2 and MMP-9 activities in mice with COPD. **A-B.** MMP-2 and MMP-9 activities of mouse lung tissues measured by gelatin zymography. **C.** Serum levels of MMP-2 and MMP-9 in the mice tested by ELISAs; * P<0.05 compared with the normal group and the 50 mg/kg JQ1 group; # P<0.05 compared with the COPD group; & P<0.05 compared with the 15 mg/kg JQ1 + COPD group; @ P<0.05 compared with the 25 mg/kg JQ1 + COPD group.
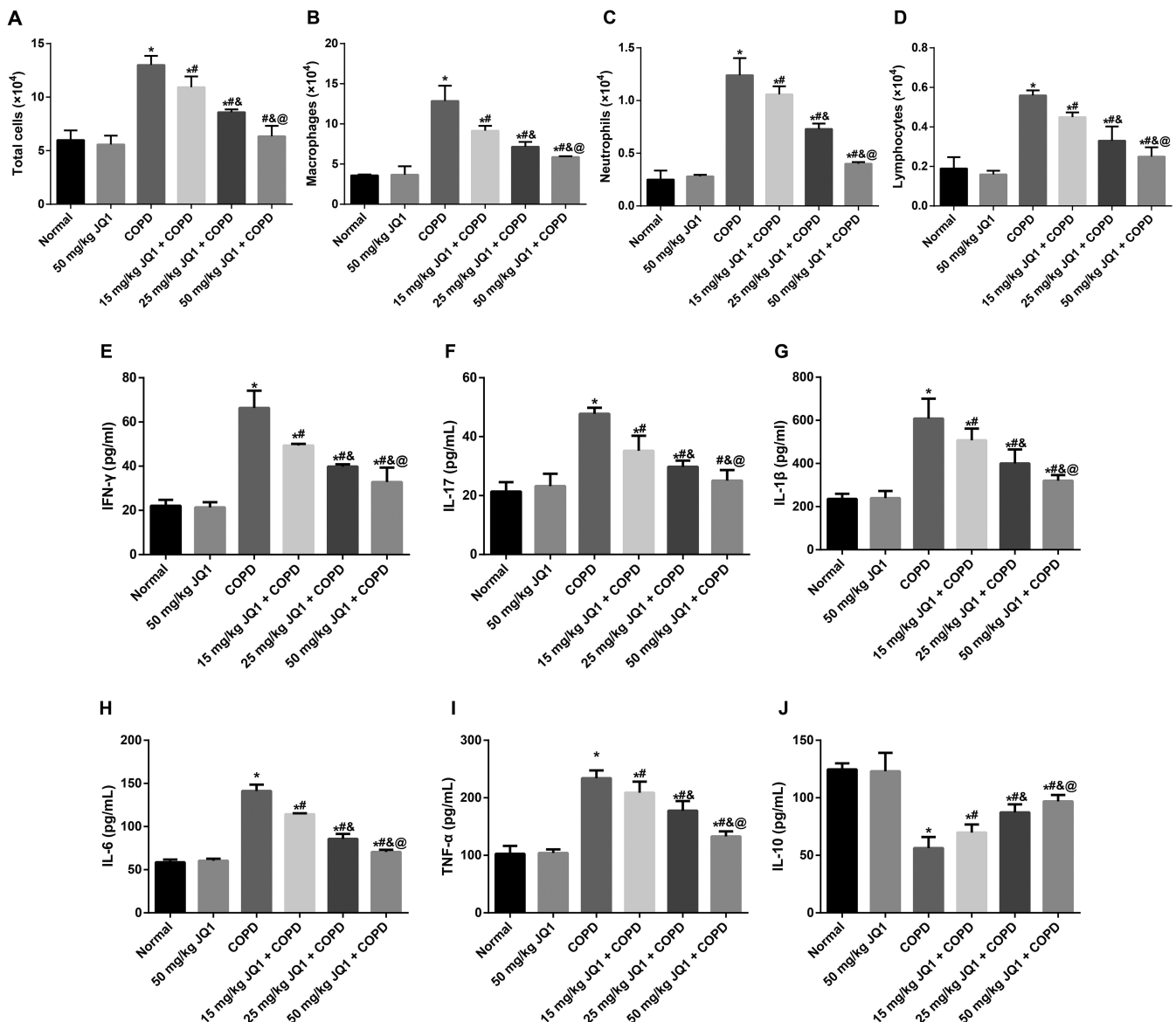
COPD, while the anti-inflammatory factor IL-10 was downregulated dramatically (all P<0.05). However, with JQ1 treatment, the IFN-γ, IL-17, IL-1β, IL-6 and TNF-α levels decreased, while the IL-10 levels increased significantly in a dose-dependent manner (all P<0.05).

JQ1 reduces oxidative stress in the mice with COPD

We detected the serum levels of oxidative stress indicators (MDA, SOD, HO-1 and T-AOC) of the mice

in each group (Fig. 6) and found a significant upregulation of MDA and obvious downregulation of SOD, HO-1 and T-AOC in the COPD model mice (all P<0.05). In addition, JQ1 effectively alleviated the oxidative stress of the mice with COPD, and the difference among the JQ1 treatment groups was statistically significant (all P<0.05). Moreover, the MDA, HO-1 and T-AOC levels in the normal group and the 50 mg/kg JQ1+COPD group did not significantly differ from each other, but the mice in the 50 mg/kg

Fig. 5. JQ1 reduces leukocytes and inflammatory cytokines in the BALF of mice with COPD. **A-D.** Quantification of total cells **(A)**, macrophages **(B)**, neutrophils **(C)**, and lymphocytes **(D)** in BALF. **E-J.** Comparison of IFN-γ **(E)**, IL-17 **(F)**, IL-1β **(G)**, IL-6 **(H)**, TNF-α **(I)** and IL-10 **(J)** levels in BALF of mice measured by ELISAs; *: P<0.05 compared with the normal group and the 50 mg/kg JQ1 group; #: P<0.05 compared with the COPD group; &: P<0.05 compared with the 15 mg/kg JQ1 + COPD group; @: P<0.05 compared with the 25 mg/kg JQ1 + COPD group.

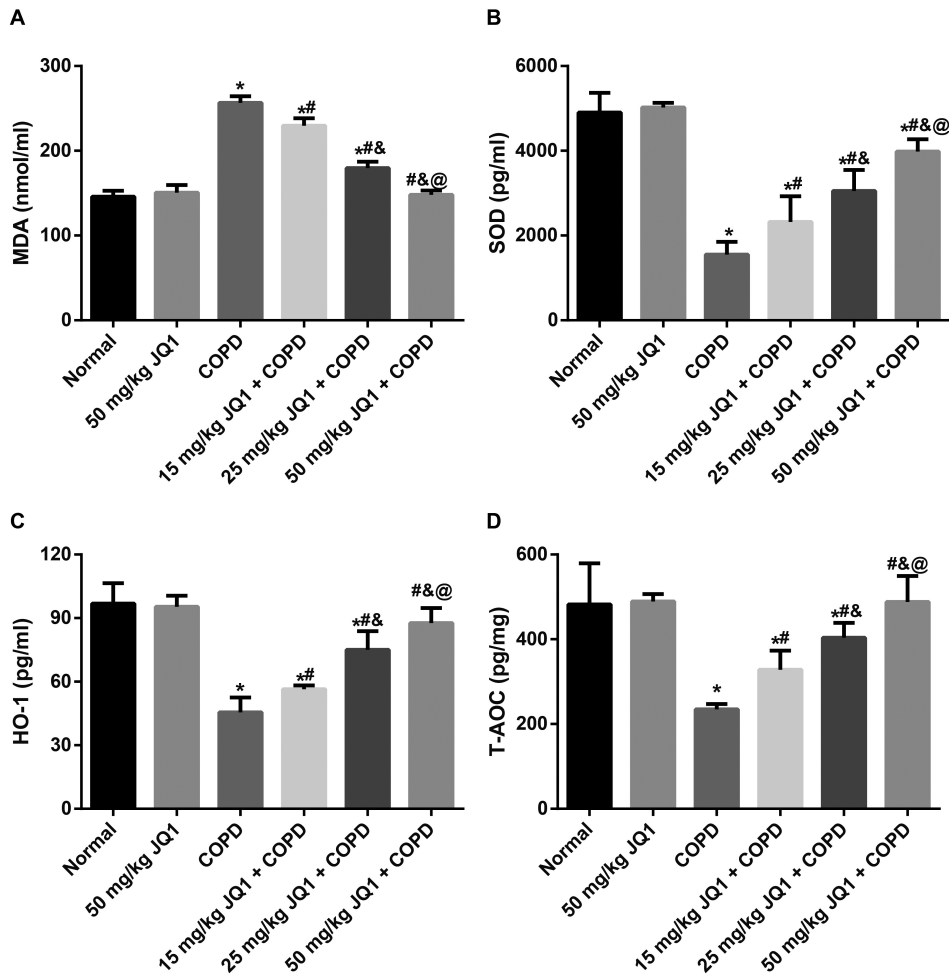JQ1+COPD group had lower SOD levels in the serum than those in the normal group (all P<0.05).

JQ1 interrupts the NF-κB signaling pathway in the lung tissues of the mice with COPD

Western blotting showed that JQ1 dose-dependently suppressed the expression of nuclear NF-κB p65 and the acetylation of NF-κB/p65 (Lys310) in the lung tissues of the mice with COPD (all P<0.05, Fig. 7A-B). Compared with the normal group, the COPD group presented apparently increased NF-κB p65/DNA binding activity in lung tissues, which can be effectively inhibited by JQ1, and the difference in NF-κB p65/DNA binding activity among the JQ1 treatment groups was significant (all P<0.05, Fig. 7C).

Discussion

Animal models have been a key factor in forming objective views regarding the pathogenesis of COPD (Wang et al., 2018). To date, researchers have developed a COPD model *in vivo* via cigarette or waterpipe smoke exposure (Alzoubi et al., 2018; Tang and Ling, 2019), cigarette smoke with porcine pancreatic elastase injection (Lu et al., 2017), or a combination of cigarette smoke and LPS with/without choline challenges (Grumelli, 2016; Wang et al., 2017; Ding et al., 2018). Smoking has been proven to be the most important risk factor and cause of COPD, and LPS plays a critical role in the acute exacerbation and progression of COPD, which replicates major aspects of *P. aeruginosa* infections in patients with severe COPD (Grumelli, 2016; Ding et al., 2018). Additionally, experiments with animal models confirmed that both cigarette smoke and LPS can promote the release of various inflammatory cytokines and the accumulation of inflammatory cells in lung tissues, giving rise to inflammation, injury and remodeling of airway and pulmonary vessels or even a decrease in lung function (Kobayashi et al., 2013; Wang et al., 2017). In the present study, we used cigarette smoke and LPS instillation to successfully establish COPD models in mice, as evidenced by the histopathological changes and measurement of

Fig. 6. Levels of oxidative stress indicators in the serum of mice in each group. Serum levels of MDA **(A)**, SOD **(B)**, HO-1 **(C)** and T-AOC **(D)**. *: P<0.05 compared with the normal group and the 50 mg/kg JQ1 group; #: P<0.05 compared with the COPD group; &: P<0.05 compared with the 15 mg/kg JQ1 + COPD group; @: P<0.05 compared with the 25 mg/kg JQ1 + COPD group.
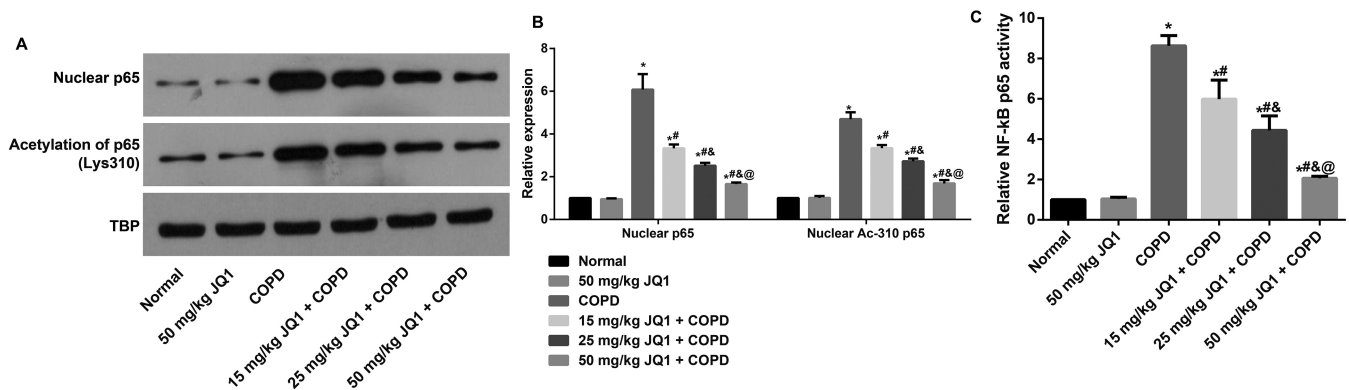
quantitative parameters.

There is evidence that smoking can enhance oxidative stress by disrupting the oxidation/antioxidation balance to directly damage lung tissues and induce autoimmune responses, thus leading to the blockage of airflow. Therefore, a new strategy for prevention and treatment of COPD is to counter oxidative stress and improve the antioxidative ability of hosts (Takimoto et al., 2012; Reynolds et al., 2016). Importantly, JQ1 treatment can reduce oxidative stress in the hippocampus of rats, accompanied by upregulation of HO-1, to attenuate diabetes-associated cognitive dysfunction (Liang et al., 2018). Younis M. Khan et al. also reported that JQ1 alleviates inflammation induced by oxidative stress in human bronchial epithelial cells (Khan et al., 2014). A recent publication showed that JQ1 could stimulate mammalian nuclear factor-erythroid 2 p45-related factor 2 (Nrf2) (Chatterjee et al., 2016), which is a central transcription factor that regulates antioxidant enzymes (including SOD, HO-1 and T-AOC) (Di Stefano et al., 2020) and MDA production (Jian et al., 2020) and acts as a modifier of several lung diseases (Barnes, 2020). The decline in Nrf2 has been linked to an increase in oxidative stress and pathogenesis in the lungs of patients with COPD (Suzuki et al., 2008). In this study, we found that JQ1 can effectively reduce MDA activity and increase SOD, HO-1 and T-AOC levels, suggesting the ability of JQ1 to alleviate oxidative stress in COPD, possibly by increasing Nrf2. To our knowledge, COPD is a very complicated chronic airway inflammation characterized by infiltration of various inflammatory cells and release of cytokines (Geraghty et al., 2017). As reported, JQ1 downregulated the expression of inflammatory cytokines, such as IL-6, IL-1β, TNF-α, and IFN-γ, thus prolonging cardiac transplant survival (Chen et al., 2020), which also downregulated the release of LPS-induced inflammatory cytokines (Das et al., 2015; Jung et al., 2015). Furthermore, JQ1 effectively inhibited the serum concentrations of Th17-associated factor (IL-17), Th1-associated factors (INF-γ and TNF-α) and Th2-associated factor (IL-6) with augmented T regulatory cell (Treg)-associated cytokines (IL-10), supporting the therapeutic value of JQ1 in lupus (Wei et al., 2015). TNF-α, mainly secreted by macrophages/monocytes, is one of the most powerful cytokines that can enhance the killing ability of neutrophils, increase the infiltration and proliferation of lymphocytes in the inflammatory site, and cause the release of other pro-inflammatory factors, including IL-6 (Samir et al., 2017). Furthermore, IL-10 released by Tregs is widely recognized, and the decreased production of IL-10 plays a pivotal role in the inflammatory exacerbation of the COPD model using cigarette smoke exposure and LPS challenge (Cervilha et al., 2019). In addition, CXCR3 knockout mice showed an inability to mount a full immune response with decreased IL-10 relative to that of WT mice after 4 weeks of smoke exposure, indicating the role of IL-10 as an anti-inflammatory and immunosuppressive cytokine in COPD (Bodger et al., 1997; Grumelli et al., 2011). In addition, Eskandarpour M et al. found that in response to JQ1, Th17-enriched cultures developed a regulatory phenotype and upregulated IL-10 secretion, suggesting that BET targeting of Th17 cells is a potential therapeutic opportunity for inflammatory and autoimmune diseases (Eskandarpour et al., 2017). In addition, increased IL-17 levels were found in the bronchoalveolar lavage fluid (BALF) of patients with COPD, followed by neutrophil recruitment during acute exacerbations induced by a *Haemophilus influenzae* infection (Roos et al., 2015). Similarly, in our study, JQ1 decreased total cells, macrophages, neutrophils, and lymphocytes in BALF with lower levels of IFN-γ, IL-17, IL-1β, IL-6 and TNF-α and higher IL-10 levels in BALF of the mice with COPD in a dose-dependent manner, suggesting that JQ1 may alleviate the inflammation of the mice with COPD by regulating the Th1/Th2 and Th17/Treg imbalance.

Fig. 7. JQ1 interrupts the NF-κB signaling pathway in the lung tissues of mice with COPD. **A-B.** Expression of nuclear NF-κB p65 and acetylation of NF-κB/p65 (Lys310) in lung tissues of mice analyzed after western blotting. **C.** NF-κB p65/DNA binding activity of lung tissues detected by the TransAMTMNF-κB p65 detection kit; *: P<0.05 compared with the normal group and the 50 mg/kg JQ1 group; #: P<0.05 compared with the COPD group; &: P<0.05 compared with the 15 mg/kg JQ1 + COPD group; @: P<0.05 compared with the 25 mg/kg JQ1 + COPD group.

Excessive accumulation of extracellular matrix (ECM), smooth muscle hyperplasia, lumen stenosis and fibrosis constitute an important pathological basis of the irreversible airflow limitation of COPD (Annoni et al., 2012). MMPs are important zinc-dependent endopeptidases that can degrade components of the ECM and are closely related to inflammation, repair and remodeling of the airway (Montano et al., 2004). By activating MMP-2 and MMP-9, BRD4 can induce the migration and invasion of HepG2 cells (Wang et al., 2015). A previous study also reported that JQ1 can inhibit the gene expression and enzyme activity of MMP in angiotensin II-induced abdominal aneurysms (Duan et al., 2016). As a member of the MMP family, MMP-2 is mainly expressed in alveolar macrophages, lymphocytes and bronchial epithelial cells, and it has been found to be highly expressed in COPD patients (Montano et al., 2004). In the pathogenesis of COPD, MMP-9 can destroy the components of the alveolar matrix, mediate the aggregation of inflammatory cells, and destroy the epithelial/endothelial structure to participate in the inflammatory response and tissue remodeling (Simpson et al., 2013). Furthermore, Grumelli S et al. revealed that macrophages downregulated MMP-9 in the lung compared to blood macrophages, indicating that MMP-9 is required for translocation to the tissue from the blood (Grumelli et al., 2019). In this study, we found that JQ1 can significantly reduce MMP-2 and MMP-9 activities in lung tissues and downregulate MMP-2 and MMP-9 levels in the serum, showing that JQ1 may regulate the expression of MMP-2 and MMP-9 to affect the degradation and synthesis of ECM, thereby playing a critical role in airway remodeling of COPD patients.

Furthermore, activation of the NF-ϰB pathway has been demonstrated to be closely related to the development and progression of COPD; therefore, NF-ϰB suppression could be a new strategy for COPD treatment (Yuan et al., 2018). Notably, Brd4 can interact with NF-ϰB p65 to affect gene transcription and regulation. For example, suppression of Brd4 leads to the downregulation of NF-ϰB transcriptional activity in Th2 cells (Zhang et al., 2012b). Moreover, JQ1 suppressed the nuclear translocation of NF-ϰB p65 in fibroblast-like synoviocytes (FLSs) isolated from the synovial tissues of RA patients in Xiao et al. (2016). Brd4 has two isomers, the short and long forms, and the carboxyl extraterminal domain (CTD) of Brd4 is identical to that of RNA polymerase II (RNA pol II), so it can interact with positive transcription elongation factor b (p-TEFb) (Itzen et al., 2014). p-TEFb is required by NF-ϰB during the transcriptional elongation of RNA pol II on the IL-8 gene (Barboric et al., 2001). Acetylation of lysine 310 is required for full transcriptional activity of p65 and activation of NF-ϰB (Chen et al., 2002). Actually, p65 acetylation on K310 can be identified by Brd4, which provides a docking site for Brd4 (Huang et al., 2009). In our study, JQ1 was discovered to dose-dependently inhibit nuclear NF-ϰB p65 expression and NF-ϰB/p65 (Lys310) acetylation in lung tissues of the mice with COPD, and it also reduced NF-ϰB p65 DNA binding activity, demonstrating a therapeutic role of JQ1 in COPD by regulating the NF-ϰB p65 pathway.

In summary, the BRD4 inhibitor JQ1 not only improves the pathological changes of lung tissues in mice with COPD, accompanied by reductions in the mean linear intercept (MLI), destructive index and inflammatory score, but also decreases MMP-2 and MMP-9 expression and alleviates oxidative stress. As such, our study supports the hypothesis that JQ1 plays a regulatory role in COPD through inhibition of the NF-ϰB pathway. However, there were several limitations in our experiment: (1) Although JQ1 is highly specific for BET family proteins, particularly BRD4 (Sakaguchi et al., 2018), its exact effect on BRD4 in COPD should be further investigated in the future; (2) the method of COPD construction may be excessively harsh to mice and exacerbate the stress response, which should be modified in future experiments.

References

Alzoubi A., Ghazwi R., Alzoubi K., Alqudah M., Kheirallah K., Khabour O. and Allouh M. (2018). Vascular endothelial growth factor receptor inhibition enhances chronic obstructive pulmonary disease picture in mice exposed to waterpipe smoke. Folia Morphol. (Warsz). 77, 447-455.

Annoni R., Lancas T., Yukimatsu Tanigawa R., de Medeiros Matsushita M., de Morais Fernezlian S., Bruno A., Fernando Ferraz da Silva L., Roughley P.J., Battaglia S., Dolhnikoff M., Hiemstra P.S., Sterk P.J., Rabe K.F. and Mauad T. (2012). Extracellular matrix composition in copd. Eur. Respir. J. 40, 1362-1373.

Barboric M., Nissen R.M., Kanazawa S., Jabrane-Ferrat N. and Peterlin B.M. (2001). NF-kappaB binds P-TEFb to stimulate transcriptional elongation by RNA polymerase II. Mol. Cell. 8, 327-337.

Barnes P.J. (2020). Oxidative stress-based therapeutics in COPD. Redox Biol. 33, 101544.

Bodger K., Wyatt J.I. and Heatley R.V. (1997). Gastric mucosal secretion of interleukin-10: Relations to histopathology, *Helicobacter pylori* status, and tumour necrosis factor-alpha secretion. Gut 40, 739-744.

Cervilha D.A.B., Ito J.T., Lourenço J.D., Olivo C.R., Saraiva-Romanholo B.M., Volpini R.A., Oliveira-Junior M.C., Mauad T., Martins M.A. and Tibério I.F.L.C. (2019). The th17/treg cytokine imbalance in chronic obstructive pulmonary disease exacerbation in an animal model of cigarette smoke exposure and lipopolysaccharide challenge association. Sci. Rep. 9, 1921.

Chatterjee N., Tian M., Spirohn K., Boutros M. and Bohmann D. (2016). Keap1-independent regulation of nrf2 activity by protein acetylation and a bet bromodomain protein. PLoS Genet. 12, e1006072.

Chen J., Miao X., Liu C., Liu B., Wu X., Kong D., Sun Q. and Gong W. (2020). BET protein inhibition prolongs cardiac transplant survival via enhanced myocardial autophagy. Transplantation 104, 2317-2326.

Chen L.F., Mu Y. and Greene W.C. (2002). Acetylation of RelA at discrete sites regulates distinct nuclear functions of NF-kappaB. EMBO J. 21, 6539-6548.

da Motta L.L., Ledaki I., Purshouse K., Haider S., De Bastiani M.A., Baban D., Morotti M., Steers G., Wigfield S., Bridges E., Li J.L., Knapp S., Ebner D., Klamt F., Harris A.L. and McIntyre A. (2017). The BET inhibitor JQ1 selectively impairs tumour response to hypoxia and downregulates CA9 and angiogenesis in triple negative breast cancer. Oncogene 36, 122-132.

Das A., Chai J.C., Yang C.S., Lee Y.S., Das N.D., Jung K.H. and Chai Y.G. (2015). Dual transcriptome sequencing reveals resistance of TLR4 ligand-activated bone marrow-derived macrophages to inflammation mediated by the BET inhibitor JQ1. Sci. Rep. 5, 16932.

Di Stefano A., Maniscalco M., Balbi B. and Ricciardolo F.L.M. (2020). Oxidative and nitrosative stress involvement in the pathogenesis of obstructive lung diseases of increasing severity. Curr. Med. Chem. 27, 7149-7158.

Ding H.B., Liu K.X., Huang J.F., Wu D.W., Chen J.Y. and Chen Q.S. (2018). Protective effect of exogenous hydrogen sulfide on pulmonary artery endothelial cells by suppressing endoplasmic reticulum stress in a rat model of chronic obstructive pulmonary disease. Biomed. Pharmacother. 105, 734-741.

Duan Q., Mao X., Liao C., Zhou H., Sun Z., Deng X., Hu Q., Qi J., Zhang G., Huang H., Plutzky J. and Yang T. (2016). Inhibition of BET bromodomain attenuates angiotensin II induced abdominal aortic aneurysm in ApoE(-/-) mice. Int. J. Cardiol. 223, 428-432.

Duan Q., McMahon S., Anand P., Shah H., Thomas S., Salunga H.T., Huang Y., Zhang R., Sahadevan A., Lemieux M.E., Brown J.D., Srivastava D., Bradner J.E., McKinsey T.A. and Haldar S.M. (2017). BET bromodomain inhibition suppresses innate inflammatory and profibrotic transcriptional networks in heart failure. Sci. Transl. Med. 9, eaah5084.

Eskandarpour M., Alexander R., Adamson P. and Calder V.L. (2017). Pharmacological inhibition of bromodomain proteins suppresses retinal inflammatory disease and downregulates retinal Th17 cells. J. Immunol. 198, 1093-1103.

Fang L.W., Bao H.L., Wang B.H., Feng Y.J., Cong S., Wang N., Fan J. and Wang L.H. (2018). A summary of item and method of national chronic obstructive pulmonary disease surveillance in china. Zhonghua Liu Xing Bing Xue Za Zhi. 39, 546-550 (in Chinese).

Ge Z., Yang Y., Zhou X., Zhang J., Li B., Wang X. and Luo X. (2019). Overexpression of the hyperplasia suppressor gene inactivates airway fibroblasts obtained from a rat model of chronic obstructive pulmonary disease by inhibiting the wnt signaling pathway. Mol. Med. Rep. 20, 2754-2762.

Geraghty P., Hadas E., Kim B.H., Dabo A.J., Volsky D.J. and Foronjy R. (2017). HIV infection model of chronic obstructive pulmonary disease in mice. Am. J. Physiol. Lung Cell Mol. Physiol. 312, L500-L509.

Grumelli S. (2016). Choline triggers exacerbations of chronic obstructive pulmonary disease in patients infected with pseudomonas aeruginosa. Curr. Respir. Med. Rev. 12, 167-174.

Grumelli S., Lu B., Peterson L., Maeno T. and Gerard C. (2011). CD46 protects against chronic obstructive pulmonary disease. PLoS One 6, e18785.

Grumelli S., Pinto-Plata V. and Celli B. (2019). Genetic switches between cancer and emphysema resolution of cigarette-smoke induced inflammation EC Pulmonol. Respir. Med. 8, 01-14.

Hassan R., Tammam S.N., Safy S.E., Abdel-Halim M., Asimakopoulou A., Weiskirchen R. and Mansour S. (2019). Prevention of hepatic stellate cell activation using JQ1- and atorvastatin-loaded chitosan nanoparticles as a promising approach in therapy of liver fibrosis. Eur. J. Pharm. Biopharm. 134, 96-106.

Huang B., Yang X.D., Zhou M.M., Ozato K. and Chen L.F. (2009). Brd4 coactivates transcriptional activation of NF-kappaB via specific binding to acetylated rela. Mol. Cell Biol. 29, 1375-1387.

Itzen F., Greifenberg A.K., Bosken C.A. and Geyer M. (2014). Brd4 activates P-TEFb for RNA polymerase II CTD phosphorylation. Nucleic Acids Res. 42, 7577-7590.

Jian T., Ding X., Li J., Wu Y., Ren B., Li J., Lv H., Chen J. and Li W. (2020). Triterpene acids of loquat leaf improve inflammation in cigarette smoking induced COPD by regulating AMPK/Nrf2 and NFkappaB pathways. Nutrients 12, 657.

Jung K.H., Das A., Chai J.C., Kim S.H., Morya N., Park K.S., Lee Y.S. and Chai Y.G. (2015). RNA sequencing reveals distinct mechanisms underlying bet inhibitor JQ1-mediated modulation of the LPS-induced activation of BV-2 microglial cells. J. Neuroinflammation 12, 36.

Kedaigle A.J., Reidling J.C., Lim R.G., Adam M., Wu J., Wassie B., Stocksdale J.T., Casale M.S., Fraenkel E. and Thompson L.M. (2020). Treatment with JQ1, a BET bromodomain inhibitor, is selectively detrimental to R6/2 Huntington's disease mice. Hum. Mol. Genet. 29, 202-215.

Khan Y.M., Kirkham P., Barnes P.J. and Adcock I.M. (2014). Brd4 is essential for IL-1beta-induced inflammation in human airway epithelial cells. PLoS One 9, e95051.

Kobayashi S., Fujinawa R., Ota F., Kobayashi S., Angata T., Ueno M., Maeno T., Kitazume S., Yoshida K., Ishii T., Gao C., Ohtsubo K., Yamaguchi Y., Betsuyaku T., Kida K. and Taniguchi N. (2013). A single dose of lipopolysaccharide into mice with emphysema mimics human chronic obstructive pulmonary disease exacerbation as assessed by micro-computed tomography. Am. J. Respir. Cell Mol. Biol. 49, 971-977.

Leal A.S., Williams C.R., Royce D.B., Pioli P.A., Sporn M.B. and Liby K.T. (2017). Bromodomain inhibitors, JQ1 and I-BET 762, as potential therapies for pancreatic cancer. Cancer Lett. 394, 76-87.

Liang E., Ma M., Wang L., Liu X., Xu J., Zhang M., Yang R. and Zhao Y. (2018). The BET/BRD inhibitor JQ1 attenuates diabetes-induced cognitive impairment in rats by targeting Nox4-Nrf2 redox imbalance. Biochem Biophys. Res. Commun. 495, 204-211.

Lu J.J., Wang Q., Xie L.H., Zhang Q. and Sun S.H. (2017). Tumor necrosis factor-like weak inducer of apoptosis regulates quadriceps muscle atrophy and fiber-type alteration in a rat model of chronic obstructive pulmonary disease. Tob. Induc. Dis. 15, 43.

Lv B., Li J., Li M., Zhuo Y., Ren K., Li E. and Yang G. (2018). Enhancement of adenovirus infection and adenoviral vector-mediated gene delivery by bromodomain inhibitor JQ1. Sci. Rep. 8, 11554.

Mason T.J. and Matthews M. (2012). Aquatic environment, housing, and management in the eighth edition of the guide for the care and use of laboratory animals: Additional considerations and recommendations. J. Am. Assoc. Lab. Anim. Sci. 51, 329-332.

Mercken E.M., Hageman G.J., Langen R.C., Wouters E.F. and Schols A.M. (2011). Decreased exercise-induced expression of nuclear

factor-kappaB-regulated genes in muscle of patients with COPD. Chest 139, 337-346.

Montano M., Beccerril C., Ruiz V., Ramos C., Sansores R.H. and Gonzalez-Avila G. (2004). Matrix metalloproteinases activity in COPD associated with wood smoke. Chest 125, 466-472.

Mumby S., Gambaryan N., Meng C., Perros F., Humbert M., Wort S.J. and Adcock I.M. (2017). Bromodomain and extra-terminal protein mimic JQ1 decreases inflammation in human vascular endothelial cells: Implications for pulmonary arterial hypertension. Respirology 22, 157-164.

Park S., Willingham M.C., Qi J. and Cheng S.Y. (2018). Metformin and JQ1 synergistically inhibit obesity-activated thyroid cancer. Endocr. Relat Cancer. 25, 865-877.

Qu M., Zhang X., Hu X., Dong M., Pan X., Bian J. and Zhou Q. (2018). BRD4 inhibitor JQ1 inhibits and reverses mechanical injury-induced corneal scarring. Cell Death Discov. 4, 5.

Reynolds C.L., Zhang S., Shrestha A.K., Barrios R. and Shivanna B. (2016). Phenotypic assessment of pulmonary hypertension using high-resolution echocardiography is feasible in neonatal mice with experimental bronchopulmonary dysplasia and pulmonary hypertension: A step toward preventing chronic obstructive pulmonary disease. Int. J. Chron. Obstruct. Pulmon Dis. 11, 1597-1605.

Rodrigo G.J. and Neffen H. (2017). A systematic review with meta-analysis of fluticasone furoate/vilanterol combination for the treatment of stable COPD. Pulm. Pharmacol. Ther. 42, 1-6.

Roos A.B., Sethi S., Nikota J., Wrona C.T., Dorrington M.G., Sanden C., Bauer C.M., Shen P., Bowdish D., Stevenson C.S., Erjefalt J.S. and Stampfli M.R. (2015). IL-17a and the promotion of neutrophilia in acute exacerbation of chronic obstructive pulmonary disease. Am. J. Respir. Crit. Care Med. 192, 428-437.

Sakaguchi T., Yoshino H., Sugita S., Miyamoto K., Yonemori M., Osako Y., Meguro-Horike M., Horike S.I., Nakagawa M. and Enokida H. (2018). Bromodomain protein BRD4 inhibitor JQ1 regulates potential prognostic molecules in advanced renal cell carcinoma. Oncotarget 9, 23003-23017.

Sakai H., Horiguchi M., Akita T., Ozawa C., Hirokawa M., Oiso Y., Kumagai H., Takeda Y., Tachibana I., Maeda N. and Yamashita C. (2017). Effect of 4-[(5,6,7,8-tetrahydro-5,5,8,8-tetramethyl-2-naphthalenyl)carbamoyl]benzoic acid (Am80) on alveolar regeneration in adiponectin deficient-mice showing a chronic obstructive pulmonary disease-like pathophysiology. J. Pharmacol. Exp. Ther. 361, 501-505.

Samir M., Glister C., Mattar D., Laird M. and Knight P.G. (2017). Follicular expression of pro-inflammatory cytokines tumour necrosis factor-alpha (TNFalpha), interleukin 6 (IL6) and their receptors in cattle: TNFalpha, IL6 and macrophages suppress thecal androgen production *in vitro*. Reproduction 154, 35-49.

Simpson J.L., McDonald V.M., Baines K.J., Oreo K.M., Wang F., Hansbro P.M. and Gibson P.G. (2013). Influence of age, past smoking, and disease severity on TLR2, neutrophilic inflammation, and MMP-9 levels in COPD. Mediators Inflamm. 2013, 462934.

Sun L., Liu J., Yuan Y., Zhang X. and Dong Z. (2018). Protective effect of the BET protein inhibitor JQ1 in cisplatin-induced nephrotoxicity. Am. J. Physiol. Renal. Physiol. 315, F469-F478.

Suzuki M., Betsuyaku T., Ito Y., Nagai K., Nasuhara Y., Kaga K., Kondo S. and Nishimura M. (2008). Down-regulated NF-E2-related factor 2 in pulmonary macrophages of aged smokers and patients with chronic obstructive pulmonary disease. Am. J. Respir. Cell Mol. Biol. 39, 673-682.

Takimoto T., Yoshida M., Hirata H., Kashiwa Y., Takeda Y., Goya S., Kijima T., Kumagai T., Tachibana I. and Kawase I. (2012). 4-hydroxy-2-nonenal induces chronic obstructive pulmonary disease-like histopathologic changes in mice. Biochem. Biophys Res. Commun. 420, 84-90.

Tang F. and Ling C. (2019). Curcumin ameliorates chronic obstructive pulmonary disease by modulating autophagy and endoplasmic reticulum stress through regulation of SIRT1 in a rat model. J. Int. Med. Res. 47, 4764-4774.

Tang K., Zhao J., Xie J. and Wang J. (2019). Decreased mir-29b expression is associated with airway inflammation in chronic obstructive pulmonary disease. Am. J. Physiol. Lung Cell. Mol. Physiol. 316, L-621-L629.

Wang G., Mohammadtursun N., Sun J., Lv Y., Jin H., Lin J., Kong L., Zhao Z., Zhang H. and Dong J. (2018). Establishment and evaluation of a rat model of sidestream cigarette smoke-induced chronic obstructive pulmonary disease. Front. Physiol. 9, 58.

Wang X.L., Li T., Li J.H., Miao S.Y. and Xiao X.Z. (2017). The effects of resveratrol on inflammation and oxidative stress in a rat model of chronic obstructive pulmonary disease. Molecules 22, 1529.

Wang Y., Xue C., Dong F., Peng Y., Zhang Y., Jin M., Zang B. and Tan L. (2014). Hydroxysafflor yellow a attenuates small airway remodeling in a rat model of chronic obstructive pulmonary disease. Biol. Pharm. Bull. 37, 1591-1598.

Wang Y.H., Sui X.M., Sui Y.N., Zhu Q.W., Yan K., Wang L.S., Wang F. and Zhou J.H. (2015). BRD4 induces cell migration and invasion in HCC cells through MMP-2 and MMP-9 activation mediated by the sonic hedgehog signaling pathway. Oncol. Lett. 10, 2227-2232.

Wei S., Sun Y. and Sha H. (2015). Therapeutic targeting of BET protein BRD4 delays murine lupus. Int. Immunopharmacol. 29, 314-319.

Xiao Y., Liang L., Huang M., Qiu Q., Zeng S., Shi M., Zou Y., Ye Y., Yang X. and Xu H. (2016). Bromodomain and extra-terminal domain bromodomain inhibition prevents synovial inflammation via blocking IkappaB kinase-dependent NF-kappaB activation in rheumatoid fibroblast-like synoviocytes. Rheumatology (Oxford) 55, 173-184.

Xiao Z., Shu J., Zhou F. and Han Y. (2018). JQ1 is a potential therapeutic option for COPD patients with agrin overexpression. Am. J. Physiol. Lung Cell Mol. Physiol. 314, L690-L694.

Yuan J., Liu R., Ma Y., Zhang Z. and Xie Z. (2018). Curcumin attenuates airway inflammation and airway remolding by inhibiting NF-kappaB signaling and COX-2 in cigarette smoke-induced COPD mice. Inflammation 41, 1804-1814.

Zhang C., Feng L., Li M., Dong C. and Zhang W. (2012a). Effects of xiaoqinglong decoction on gene expression profiles in a rat chronic obstructive pulmonary disease model. Biosci. Trends. 6, 262-269.

Zhang G., Liu R., Zhong Y., Plotnikov A.N., Zhang W., Zeng L., Rusinova E., Gerona-Nevarro G., Moshkina N., Joshua J., Chuang P.Y., Ohlmeyer M., He J.C. and Zhou M.M. (2012b). Down-regulation of NF-kappaB transcriptional activity in HIV-associated kidney disease by BRD4 inhibition. J. Biol. Chem. 287, 28840-28851.